Commun. Comput. Phys.
doi: 10.4208/cicp.181113.271114a

Vol. **17**, No. 3, pp. 703-720
March 2015

A Multilevel Numerical Approach with Application in Time-Domain Electromagnetics

Avijit Chatterjee*

Department of Aerospace Engineering, Indian Institute of Technology, Bombay, Mumbai 400076, India.

Received 18 November 2013; Accepted (in revised version) 27 November 2014

Communicated by Wei Cai

Abstract. An algebraic multilevel method is proposed for efficiently simulating linear wave propagation using higher-order numerical schemes. This method is used in conjunction with the Finite Volume Time Domain (FVTD) technique for the numerical solution of the time-domain Maxwell's equations in electromagnetic scattering problems. In the multilevel method the solution is cycled through spatial operators of varying orders of accuracy, while maintaining highest-order accuracy at coarser approximation levels through the use of the relative truncation error as a forcing function. Higher-order spatial accuracy can be enforced using the multilevel method at a fraction of the computational cost incurred in a conventional higher-order implementation. The multilevel method is targeted towards electromagnetic scattering problems at large electrical sizes which usually require long simulation times due to the use of very fine meshes dictated by point-per-wavelength requirements to accurately model wave propagation over long distances.

AMS subject classifications: 35L05, 74J05, 78A45, 778A45, 76M12

Key words: Finite volume, time-domain, Maxwell's equations, scattering, multilevel, higher-order.

1 Introduction

Higher-order accurate spatial approximations of partial differential equations (PDEs) are considered necessary in numerical simulations seeking to resolve complex spatial physical phenomena. In principle complex spatial phenomena can be numerically captured with lower-order accurate approximations, but in practice it is often prohibitively expensive to do so because of the large number of grid points required to obtain requisite resolution while operating with lower-order techniques. For numerical simulation of

*Corresponding author. *Email address:* avijit@aero.iitb.ac.in (A. Chatterjee)

 ©2015 Global-Science Press

https://doi.org/10.4208/cicp.181113.271114a Published online by Cambridge University Press

scattering problems in time-domain electromagnetics, a basic mesh resolution expressed in terms of points-per-wavelength (PPW) is usually required to adequately resolve the physical process. This mesh resolution stems mainly from the need to accurately model wave propagation both in terms of phase and amplitude over long distances in electromagnetic scattering problems especially at large electrical sizes [1, 2]. The overall mesh size is then dictated by the the electrical size of the problem based on the ratio of the characteristic length of the scatterer and the wavelength of the incident radiation. Numerical techniques like finite difference time domain (FDTD) and finite volume time domain (FVTD) methods are based on directly solving the time domain Maxwell's equations, and face serious difficulties in simulating electromagnetic scattering from electrically large scatterers due to the requirement of long computational times directly related to the fine discretization dictated by PPW requirements [1,3]. Higher-order accurate spatial approximations are usually employed to model the time domain Maxwell's equations with far fewer grid points due to a more relaxed PPW requirement compared to a lower first-order method. This often leads to a reduction in overall computational cost due to a significant decrease in mesh size despite being much costlier on a per-grid-point basis [1, 4]. There have not been many instances in literature of successful advances at an algorithm level to accelerate FDTD or FVTD based numerical simulations to offset this disadvantage of long simulation times at large electrical sizes. The time domain Maxwell's equations solved by FDTD and FVTD methods are a set of linear hyperbolic PDEs, which in the case of the FVTD technique is posed as a set of hyperbolic conservation laws. The multigrid technique [5] in which the solution is cycled through a hierarchy of grids from fine to coarse has been very successful in accelerating convergence of boundary value problems. The multigrid technique initially introduced to solve the system of linear algebraic equations resulting from discretizing linear elliptic PDEs, are based on the efficient smoothing of high frequency error components relative to the discretization in hand. The multigrid method, in the full approximation scheme (FAS) [6] form also applicable to nonlinear problems, uses the relative local truncation error (τ) between finer and coarser grids as a forcing function for coarse grid calculations, in order to maintain fine-grid accuracy for the coarse grid computed solution. The relative truncation error, but between higher and lower order accurate spatial approximations, is also used in defect correction techniques to obtain less expensively higher (usually second) order accuracy by appropriately forcing the lower-order calculation. The concept of τ extrapolation [6] can also be applied to suitably modify the relative truncation error enforced on coarse grid calculations in the multigrid process to get an even higher order accurate approximation on the coarse grid than exists on the finer grid. The original geometric multigrid method based on efficient smoothing of high frequency error components on successive coarser discretizations has been extended, especially in the case of finite element based higher-order discontinuous Galerkin (DG) methods, to the polynomial order or p-multigrid framework based on successive coarser approximations on a fixed discretization. In the p-multigrid method, lower-order polynomial approximations serve as the coarser levels where again high frequency error components are efficiently sought to be smoothed out [7].

https://doi.org/10.4208/cicp.181113.271114a Published online by Cambridge University Press

The arguments for the extension of multigrid methods to hyperbolic PDEs often have a heuristic basis and rely on numerical solvers for convection dominated problems having error smoothing properties more typical in iterative solvers solving boundary value problems. FDTD and FVTD methods are normally based on explicit time-stepping and suffer from time step restrictions due to stability considerations while solving the time-domain Maxwell's equations. For electromagnetic scattering from electrically large scatterers, a PPW requirement usually between 10 and 20, can result in a very fine grid with large number of grid points and a very small time step. Numerical simulations, in addition, may be required to run in excess of 40 sinusoidal time cycles for electrically large three dimensional scatterers with re-entrant structures resulting in extremely large simulation times [9]. Geometric multigrid methods are not as efficient in dealing with dispersion related errors associated with convection dominated problems on coarser levels [10], and this can also limit the number of coarse grid levels that can be traversed in the multigrid process [11]. In the current work, an algebraic multilevel approach is proposed for accelerating explicit time-stepping based FVTD simulations for electromagnetic scattering problems. The method seeks to efficiently exploit the general ability [1, 2] of a spatially higher-order accurate method, to more accurately model wave propagation over long distances on a relatively coarse but fixed mesh. As in the mostly finite element based p-multigrid method, the hyperbolic PDE in terms of the time-domain Maxwell's equations, are discretized using spatial operators of varying orders of accuracy on a fixed grid and the solution cycled through the different spatially accurate representations from highest to lowest. But unlike the p-multigrid method which relies on efficient smoothing of error components at coarser approximation levels to achieve an accelerated steady state of mainly nonlinear problems, the present algebraic multilevel method is based on higher-order spatially accurate approximations to sufficiently smooth solutions of the linear hyperbolic PDE being inexpensively maintained at coarser approximation levels in a purely advection process which characterizes solution of time-domain Maxwell's equations in a electromagnetic scattering problem. Higher-order accuracy at coarser approximation levels is achieved via an appropriate correction term based on the relative truncation error τ in the purely advection process of linear wave propagation. This is proven for the simple case of scalar advection equation on two levels and implemented for a system of linear hyperbolic conservation laws, describing wave propagation in electromagnetic scattering problems, using a higher-order characteristic based finite volume technique. The algebraic multilevel method easily blends with a standard higher-order finite volume frameworks, does not require any prolongation or restriction operations while traversing different approximation levels and is also able to maintain transient accuracy while reaching an accelerated steady state. The multilevel method is used in conjunction with the higher-order FVTD technique to predict electromagnetic scattering from two-dimensional (2D) perfect conducting bodies at a fraction of the computational cost of a conventional higher-order implementation and at costs comparable to that for lower-order operators.

https://doi.org/10.4208/cicp.181113.271114a Published online by Cambridge University Press

2 Algebraic multilevel method

The well known FAS introduced by Brandt [6,8] extends the original geometric multigrid method for accelerating the numerical solution linear boundary value problems to nonlinear ones. Assuming the problem to be solved on the fine grid Ω^h, of a two-grid process to be represented by

$$A^h\mathbf{u}^h = \mathbf{f}^h, \tag{2.1}$$

then the coarse grid problem to be solved on the coarser grid Ω^H in the FAS can be written in the standard form as

$$A^H\mathbf{u}^H = A^H(\mathbf{v}^H) + \mathbf{r}^H, \tag{2.2}$$

with $\mathbf{r}^H$ the restricted form of the fine-grid residual on the coarse grid defined as

$$\mathbf{r}^H = I_h^H(\mathbf{f^h} - \mathbf{A^h}(\mathbf{v^h})). \tag{2.3}$$

Here A represents the possibly nonlinear operator, $\mathbf{v}^h$ approximates the actual solution $\mathbf{u}^h$ prior to commencing coarse-grid operations, I_h^H indicates a generic restriction operator from the fine to coarse grid and $\mathbf{v}^H = I_h^H\mathbf{v}^h$. After solving on the coarse grid the current fine-grid approximation is updated as

$$\mathbf{v}^h \leftarrow \mathbf{v}^h + I_H^h(\mathbf{u}^H - \mathbf{v}^H), \tag{2.4}$$

with I_H^h the prolongation operator from coarse to fine grid. If A is a linear operator, the FAS is identical to the classical coarse-grid correction scheme on two grids for linear problems. FAS is usually applied recursively to incorporate more coarser levels in the course of a multigrid cycle [6,8]. An alternative view of the FAS emerges [5] by rewriting Eq. (2.2) as

$$A^H\mathbf{u}^H = \mathbf{f}^H + \boldsymbol{\tau}_H^h, \tag{2.5}$$

where

$$\mathbf{f}^H = I_h^H\mathbf{f}^h \tag{2.6}$$

and

$$\boldsymbol{\tau}_H^h = A^H(I_h^H\mathbf{v}^h) - I_h^H A^h(\mathbf{v}^h) \tag{2.7}$$

is interpreted as the fine-to-coarse defect correction or the relative local truncation error between the two discretizations. $\boldsymbol{\tau}_H^h$ is essentially a correction to the coarse grid equation designed to make the converged solution coincide with the fine-grid solution so that at convergence $\mathbf{u}^H = I_h^H\mathbf{u}^h$. This latter interpretation of the FAS has inspired many defect correction methods along with p-multigrid approaches [7] in the DG framework. This interpretation of the FAS can also be considered the building block for the proposed algebraic multilevel method dealing with problems of linear wave propagation. The relative truncation error is used to force calculations at lower spatial approximation levels to ensure spatial accuracy of the highest approximation at all subsequent lower levels. This is described next for a scalar linear wave equation and then extended to a system of linear hyperbolic PDEs.

https://doi.org/10.4208/cicp.181113.271114a Published online by Cambridge University Press

2.1 Scalar law

We initially consider the simplest case of a multilevel method with only two levels involving second and first-order spatial approximations for the numerical solution of the scalar advection equation. The solution is cycled between second-order and first-order accurate spatial operators. Second-order spatial accuracy is sought be enforced at the coarser first-order approximation through the use of an appropriate forcing function based on the relative truncation error between the second and first-order approximation levels in a FAS [6] framework. The scalar linear advection equation is represented by

$$u_t + a u_x = 0 \tag{2.8}$$

with $a \geq 0$. We assume the scalar advection equation being solved on an uniform grid by an explicit numerical scheme characterized spatially solely by its numerical flux function. Let $\mathcal{F}^n_{p,i+1/2}$ denote the numerical flux function for a p^{th} order spatially accurate approximation of the PDE at spatial location $x_{i+1/2}$ representing the cell face between nodes i and $i+1$ at time level n. For a first-order accurate upwind scheme this is expressed by

$$\mathcal{F}^n_{1,i+1/2} = a U^n_i, \tag{2.9}$$

where U^n_i is assumed to numerically approximate pointwise value $u(x_i,t_n)$. For a second-order accurate approximation, the corresponding numerical flux can be assumed to be based on a convex combination of the physical fluxes at nodes i and $i+1$ and is expressed as

$$\mathcal{F}^n_{2,i+1/2} = a(\alpha U^n_i + \beta U^n_{i+1}) \tag{2.10}$$

with $\alpha+\beta=1$. For the multilevel method, the numerical flux is represented by $\hat{\mathcal{F}}$, and for the two-level method this is evaluated at the first-order approximation level as

$$\hat{\mathcal{F}}^n_{1,i+1/2} = a U^n_i + \gamma^n_{1,i+1/2}. \tag{2.11}$$

$\gamma^n_{1,i+1/2}$ like in a FAS framework represents a forcing function based on data at time level $n-1$, applied to the first-order numerical flux function $\mathcal{F}^n_{1,i+1/2} = a U^n_i$ at time level n, in order to enforce a second-order accuracy in the two-level method when computations are transferred to the first-order approximation level from the previous second-order level at $n-1$. More specifically

$$\gamma^n_{1,i+1/2} = \mathcal{F}^{n-1}_{2,i+1/2} - \mathcal{F}^{n-1}_{1,i+1/2} = a(\alpha U^{n-1}_i + \beta U^{n-1}_{i+1}) - a U^{n-1}_i \tag{2.12}$$

and Eq. (2.11) is rewritten as

$$\hat{\mathcal{F}}^n_{1,i+1/2} = a U^n_i - a U^{n-1}_i + a(\alpha U^{n-1}_i + \beta U^{n-1}_{i+1}). \tag{2.13}$$

It may be mentioned that the more familiar form of relative truncation error τ in a finite-volume context, is defined cellwise as the difference of residuals. Thus, $\tau^n_{p,i}$ the relative truncation error defined at the p^{th} approximation level for the cell i is simply

$$\tau^n_{p,i} = (\gamma^n_{p,i+1/2} - \gamma^n_{p,i-1/2})/\Delta x. \tag{2.14}$$

https://doi.org/10.4208/cicp.181113.271114a Published online by Cambridge University Press

The two-level method returns exactly a second-order accurate solution while operating at the first-order approximation level if

$$\hat{\mathcal{F}}_{1,i+1/2} = \mathcal{F}_{2,i+1/2}. \tag{2.15}$$

To impose conditions on the true solution of the PDE $u(x,t)$ for this to be valid, Eqs. (2.10) and (2.13) for numerical fluxes are written using the exact solution of the linear advection equation. The numerical fluxes in terms of the exact solution are as follows

$$\hat{\mathcal{F}}^n_{1,i+1/2} = a[u(x,t) - u(x,t-\Delta t) + \alpha u(x,t-\Delta t) + \beta u(x+\Delta x, t-\Delta t)] \tag{2.16}$$

and

$$\mathcal{F}^n_{2,i+1/2} = a[\alpha u(x,t) + \beta u(x+\Delta x,t)]. \tag{2.17}$$

Eqs. (2.16) and (2.17) are then rewritten uniformly for $t-\Delta t = \tilde{t}$, based on the assumption that $u(x,t)$ satisfies the scalar advection equation exactly and $a\Delta t = \Delta x$ as

$$\hat{\mathcal{F}}^n_{1,i+1/2} = a[u(x-\Delta x,\tilde{t}) - u(x,\tilde{t}) + \alpha u(x,\tilde{t}) + \beta u(x+\Delta x,\tilde{t})] \tag{2.18}$$

and

$$\mathcal{F}^n_{1,i+1/2} = a[\alpha u(x-\Delta x,\tilde{t}) + \beta u(x,\tilde{t})]. \tag{2.19}$$

Eq. (2.18) is further rewritten as

$$\hat{\mathcal{F}}^n_{1,i+1/2} = a[\alpha u(x-\Delta x,\tilde{t}) + (1-\alpha)u(x-\Delta x,\tilde{t}) + \beta u(x,\tilde{t}) - 2\beta u(x,\tilde{t}) + \beta u(x+\Delta x,\tilde{t})]. \tag{2.20}$$

The condition required to be satisfied by the true solution of the PDE $u(x,t)$ is obtained by equating Eqs. (2.20) and (2.19) and is

$$(1-\alpha)u(x-\Delta x,\tilde{t}) - 2\beta u(x,\tilde{t}) + \beta u(x+\Delta x,\tilde{t}) = 0. \tag{2.21}$$

Since $\alpha+\beta=1$, the above expression is

$$u(x,t) = [u(x-\Delta x,t) + u(x+\Delta x,t)]/2, \tag{2.22}$$

which in continuous space is interpreted, in the limit $\Delta x \to 0$, as a condition of differentiability for $u(x,t)$. Thus, the two level method involving first and second-order approximations can be expected to exactly return a second-order accurate solution in a FAS framework if the true solution of the PDE satisfies conditions of sufficient smoothness indicated here by requiring the true solution to be differentiable in space.

2.2 System of equations

The previous analysis for the scalar advection equation can be naturally extended to a system of linear equations by considering individual scalar advection equations obtained

https://doi.org/10.4208/cicp.181113.271114a Published online by Cambridge University Press

by decoupling the original system of hyperbolic conservation laws. Consider the system of a M linear hyperbolic conservation laws simply given by

$$\mathbf{u}_t + \hat{A}\mathbf{u}_x = 0. \tag{2.23}$$

Defining $\mathbf{w}$ to be the vector of characteristic variables with $\mathbf{w} = R^{-1}\mathbf{u}$, where R is the matrix of right eigenvectors of the Jacobian matrix $\hat{A}$, the system of equations in Eq. (2.23) decouples to M independent scalar advection equations

$$(w_q)_t + \lambda_q (w_q)_x = 0 \tag{2.24}$$

with $q = 1, M$ and λ_q the eigenvalues of $\hat{A}$. Thus, the analysis for scalar advection equation in the previous section is applicable to each individual scalar equation in Eq. (2.24) advecting with speed given by the appropriate eigenvalue. For characteristic based numerical schemes like that used in the present work, this analysis valid for independent scalar advection equations arising from decoupling the original linear hyperbolic system in Eq. (2.23), blends smoothly even in the numerical framework.

2.3 Multidimensional system of equations on multilevels

The multilevel method can be formalized and naturally extended to a multidimensional system of linear hyperbolic conservation laws on multiple levels for sufficiently smooth solutions $\boldsymbol{u}(\mathbf{r},t)$ of the linear hyperbolic time-dependent PDE being numerically solved. We consider a two-dimensional system of time-dependent linear hyperbolic conservation laws given by

$$\frac{\partial \boldsymbol{u}}{\partial t} + \frac{\partial \boldsymbol{f}(\boldsymbol{u})}{\partial x} + \frac{\partial \boldsymbol{g}(\boldsymbol{u})}{\partial y} = \boldsymbol{s} \tag{2.25}$$

integrating the differential form of the conservation law, represented by Eq. (2.25) over an arbitrary control volume Ω

$$\frac{\partial \int_\Omega \boldsymbol{u} d\mathcal{V}}{\partial t} + \int_\Omega \boldsymbol{\nabla}.(\boldsymbol{F}(\boldsymbol{u}))d\mathcal{V} = 0, \tag{2.26}$$

where $\mathbf{F}$ is the flux vector with components $\mathbf{f}$,$\mathbf{g}$ in the Cartesian x,y directions. The source term $\mathbf{s}$ is assumed to be zero for simplification. In the finite volume approximation the integral form of the conservation law to be discretized is obtained by applying the divergence theorem as

$$\frac{\partial \int_\Omega \boldsymbol{u} d\mathcal{V}}{\partial t} + \oint_{\mathcal{S}} \boldsymbol{F}(\boldsymbol{u}).\hat{\boldsymbol{n}} d\mathcal{S} = 0 \tag{2.27}$$

with $\hat{\boldsymbol{n}}$ the outward unit normal vector. The two-dimensional spatially discretized form, also numerically solved for in the present work, can be finally written as [11, 12]

$$A_k \frac{d\boldsymbol{U}_k}{dt} + \sum_{j=1}^{4} [(\boldsymbol{\mathcal{F}}(\boldsymbol{U}).\hat{\boldsymbol{n}}\mathcal{S})_j]_k = 0, \tag{2.28}$$

https://doi.org/10.4208/cicp.181113.271114a Published online by Cambridge University Press

where the numerical flux $[(\boldsymbol{\mathcal{F}}(\boldsymbol{U}).\hat{\boldsymbol{n}}\mathcal{S})_j]_k$ approximates the average flux through face j of cell k and A_k represents the area of the quadrilateral cells in structured discretized 2D space. The semi-discrete form in Eq. (2.28) with a p^{th} order spatially accurate discretization is written in a conventional (single-level) residual form as

$$\frac{d\boldsymbol{U}}{dt}+\boldsymbol{R}_p(\boldsymbol{U}^n)=0, \tag{2.29}$$

where superscript n indicates the time level. In the proposed algebraic multilevel method the solution is cycled through spatial approximations of varying orders of accuracy from highest to lowest. The relative truncation error (τ) between the highest and local p^{th} approximation level is used to force the highest-order approximation accuracy at the local p^{th} level. Thus, the semi-discrete form to be evaluated at the p^{th} order approximation level is

$$\frac{d\boldsymbol{U}}{dt}+\boldsymbol{R}_p(\boldsymbol{U}^n)+\boldsymbol{\tau}_p^n=0, \tag{2.30}$$

with $\boldsymbol{\tau}_p^n$ the relative truncation error between the highest and local p^{th} order approximation at the n^{th} time level can be defined as

$$\boldsymbol{\tau}_p^n=\boldsymbol{R}_{p+1}(\boldsymbol{U}^{n-1})-\boldsymbol{R}_p(\boldsymbol{U}^{n-1})+\boldsymbol{\tau}_{p+1}^{n-1}. \tag{2.31}$$

The algebraic multilevel method in its simplest form, consists of individual cycles in which a single time step is undertaken at each approximation level starting from the highest till the lowest approximation level is reached before reverting back to the highest level for the next cycle. This in principle is very similar to the sawtooth cycle for solving time-dependent nonlinear hyperbolic PDEs with a geometric multigrid method in a FAS framework [13], with each multigrid cycle consisting of a single time step executed on each mesh from finest to the coarsest with an identically defined relative truncation error across h-levels based on the relative mesh discretization. In the other multilevel variant for which results are also presented, $\nu>1$ time steps are taken at the lowest (usually first-order accurate) approximation level before returning to the highest approximation level. This has similarities with the frozen τ concept [6] proposed for geometric multigrid methods. In the frozen τ variant of the multilevel method, the semi-discrete form to be evaluated at an in-between time step $n^{'}$ with $1\leq n^{'}\leq\nu$, at the first-order approximation level is

$$\frac{d\boldsymbol{U}}{dt}+\boldsymbol{R}_1(\boldsymbol{U}^{n+n^{'}-1})+\boldsymbol{\tau}_1^n=0, \tag{2.32}$$

with the first-order level initially accessed at time level n in the cycle. It is worth noting that the sawtooth variant is simply a special case of the frozen τ implementation with $\nu=1$ and is henceforth referred to a multilevel method with $\nu=1$. As in the present work, the semi-discrete form as in Eq. (2.31) can be integrated in time using a multistage Runge-Kutta time stepping scheme. The relative truncation error $\boldsymbol{\tau}_p^n$ is calculated for each individual finite volume cell and applied as a forcing function to all stages of the Runge-Kutta time stepping at the p^{th} approximation level [13].

https://doi.org/10.4208/cicp.181113.271114a Published online by Cambridge University Press

2.4 Work flow

The algebraic multilevel framework is shown schematically in Fig. 1. The work flow for the multilevel method in its simple frozen τ variant is as follows,

- Define number of cycles = N and number of levels in each cycle = m. m is the highest spatial order of accuracy in the multilevel method. Start cycle 1 with initial value $\boldsymbol{U}^0$ at level $p=m$.

  1. At $p=m$, calculate $\boldsymbol{R}_{p=m}(\boldsymbol{U}^o)$ and obtain $\boldsymbol{U}^1$ by advancing a single time step by integrating
  $$\frac{d\boldsymbol{U}}{dt}+\boldsymbol{R}_m(\boldsymbol{U}^0)=0 \tag{2.33}$$
  in time. As mentioned in the present work a two-stage Runge-Kutta time stepping is used. Move to $p=m-1$.
  2. At $p=m-1$, calculate $\boldsymbol{R}_{p=m-1}(\boldsymbol{U}^0)$ and $\boldsymbol{R}_{p=m-1}(\boldsymbol{U}^1)$. Obtain
  $$\boldsymbol{\tau}^1_{p=m-1}=\boldsymbol{R}_{p+1}(\boldsymbol{U}^0)-\boldsymbol{R}_p(\boldsymbol{U}^0). \tag{2.34}$$
  $\boldsymbol{R}_{p+1}(\boldsymbol{U}^0)$ is available from the previous level. Advance another time step to obtain $\boldsymbol{U}^2$ by solving
  $$\frac{d\boldsymbol{U}}{dt}+\boldsymbol{R}_{m-1}(\boldsymbol{U}^1)+\boldsymbol{\tau}^1_{m-1}=0. \tag{2.35}$$
  As mentioned the forcing function is applied at each stage of the multistage Runge-Kutta time stepping. Move to $p=m-2$.

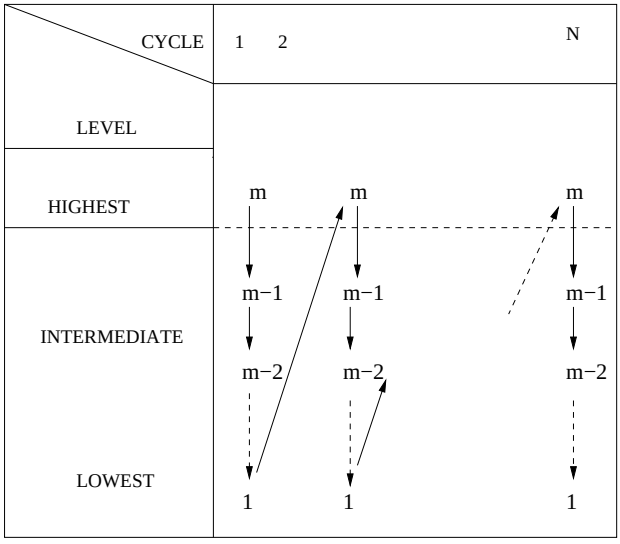


Figure 1: Multilevel method with m levels, ν time steps at the lowest level.

https://doi.org/10.4208/cicp.181113.271114a Published online by Cambridge University Press

3. At $p=m-2$, calculate $\boldsymbol{R}_{p=m-2}(\boldsymbol{U}^1)$ and $\boldsymbol{R}_{p=m-2}(\boldsymbol{U}^2)$. Obtain

$$\boldsymbol{\tau}^2_{p=m-2}=\boldsymbol{R}_{p+1}(\boldsymbol{U}^1)-\boldsymbol{R}_p(\boldsymbol{U}^1)+\boldsymbol{\tau}^1_{p+1}. \tag{2.36}$$

$\boldsymbol{\tau}^1_{p+1}$ is again available from the previous level. Advance another time step to obtain $\boldsymbol{U}^3$ by time integrating

$$\frac{d\boldsymbol{U}}{dt}+\boldsymbol{R}_{m-2}(\boldsymbol{U}^2)+\boldsymbol{\tau}^2_{m-2}=0. \tag{2.37}$$

Move to $p=m-3,\cdots$.

$\vdots$

m. At $p=1$, define ν, calculate $\boldsymbol{R}_{p=1}(\boldsymbol{U}^{m-2})$ and $\boldsymbol{R}_{p=1}(\boldsymbol{U}^{m-1})$. Obtain

$$\boldsymbol{\tau}^{m-1}_{p=1}=\boldsymbol{R}_{p+1}(\boldsymbol{U}^{m-2})-\boldsymbol{R}_p(\boldsymbol{U}^{m-2})+\boldsymbol{\tau}^{m-2}_{p+1} \tag{2.38}$$

with $\boldsymbol{R}_{p+1}(\boldsymbol{U}^{m-2})$ available from the previous level. Advance ν time step to obtain $\boldsymbol{U}^{m+\nu-1}$ by integrating

$$\frac{d\boldsymbol{U}}{dt}+\boldsymbol{R}_{p=1}(\boldsymbol{U}^{m-1})+\boldsymbol{\tau}^{m-1}_1=0 \tag{2.39}$$

for ν time steps with the fixed value of $\boldsymbol{\tau}^{m-1}_1$.

- Move to cycle 2 with initial value $\boldsymbol{U}^{m+\nu-1}$.

For a time-dependent problem advancing time T would imply

$$N=\frac{T}{\Delta t(m+\nu-1)}. \tag{2.40}$$

It is worth noting that unlike h or p-multigrid methods no prolongation or restriction operators are required in the present multilevel framework.

3 Application to time-domain electromagnetics

The 2D conservative form solved for in the present work has vectors in Eq. (2.25) for TM waves as

$$\boldsymbol{u}=\begin{pmatrix} B_x \\ B_y \\ D_z \end{pmatrix},\quad \boldsymbol{f}=\begin{pmatrix} 0 \\ -D_z/\varepsilon \\ -B_y/\mu \end{pmatrix},\quad \boldsymbol{g}=\begin{pmatrix} D_z/\varepsilon \\ 0 \\ B_x/\mu \end{pmatrix},\quad \boldsymbol{s}=\begin{pmatrix} 0 \\ 0 \\ -J_{iz} \end{pmatrix} \tag{3.1}$$

https://doi.org/10.4208/cicp.181113.271114a Published online by Cambridge University Press

while that for TE waves

$$\boldsymbol{u}=\begin{pmatrix} B_z \\ D_x \\ D_y \end{pmatrix}, \quad \boldsymbol{f}=\begin{pmatrix} D_y/\varepsilon \\ 0 \\ B_z/\mu \end{pmatrix}, \quad \boldsymbol{g}=\begin{pmatrix} -D_x/\varepsilon \\ -B_z/\mu \\ 0 \end{pmatrix}, \quad \boldsymbol{s}=\begin{pmatrix} 0 \\ -J_{ix} \\ -J_{iy} \end{pmatrix}. \tag{3.2}$$

B is the magnetic induction, **D** the electric field displacement, $\mathbf{J_i}$ the impressed current density vector with ε and μ respectively the permittivity and permeability in free space. Additionally for scattering in free space the source term **s** is identically zero. In the present work the Maxwell's equations for TM or TE waves, in its semi-discretized form in Eq. (2.28), are solved using well known higher-order ENO [14–16] based spatial discretization and a second-order Runge-Kutta time integration in a cell-centered and scattered field formulation. The ENO scheme in the ENO-Roe form [14, 15] used here efficiently implements the ENO reconstruction based on the numerical fluxes. The numerical flux function for the p^{th} order accurate ENO based spatial discretization of the one-dimension scalar hyperbolic conservation law

$$u_t+f(u)_x=0 \tag{3.3}$$

is represented by $\mathcal{F}_{p,i+1/2}$ and is expressed as

$$\mathcal{F}_{i+1/2}=\sum_{l=0}^{p-1}\alpha_{s,l}^{p}f_{i-p+1+s+l}, \tag{3.4}$$

where $\alpha_{s,l}^{p}$ are the reconstruction coefficients, and s the stencil index selected among the p candidate stencils on the basis of providing the smoothest possible approximation [15]. This is applied to the two-dimensional system of equations (2.25) by decoupling the system into three scalar hyperbolic conservation laws normal to the cell faces. Evaluation of the numerical flux function at the four cell faces leads to the general residual form of Eq. (2.29).

3.1 Numerical results

Transient as well as steady state results are presented for electromagnetic scattering from a 2D perfectly conducting circular cylinder using the multilevel method. The transient problem considered has the 2D cylinder shown in Fig. 2 illuminated by an incident TE Gaussian plane wave represented by [17]

$$\boldsymbol{H}^i(\boldsymbol{r},t)=\boldsymbol{a}_z H_o\frac{4.0}{\sqrt{\pi}T}e^{-\gamma^2}, \tag{3.5}$$

where

$$\gamma=\frac{4.0}{T}(ct-ct_o-\boldsymbol{r}\cdot\boldsymbol{a}_k) \tag{3.6}$$

https://doi.org/10.4208/cicp.181113.271114a Published online by Cambridge University Press

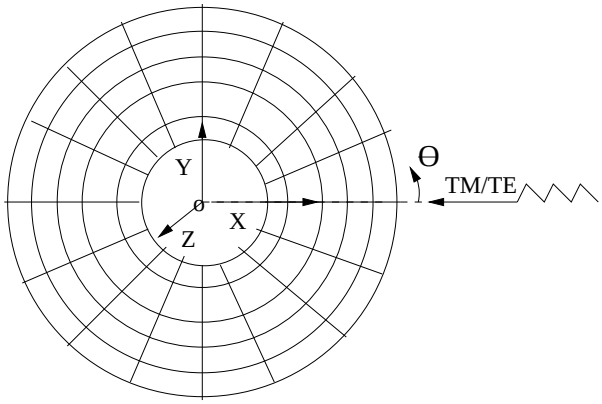


Figure 2: Grid and illumination circular cylinder, schematic.

with $\boldsymbol{r}$ the position vector with respect to the origin, $H_o = -1$, $\boldsymbol{a}_z$ the unit vector in the Cartesian z direction, $\boldsymbol{a}_k = -\boldsymbol{a}_x$ the unit vector in the direction of propagation of the incident wave, T the pulse width $= 4$ light meters (LM) and $t_o = 6$ LM. One LM is the unit of time required for the electromagnetic wave to travel 1 m in free space [17] and c the wave speed. The cylinder of diameter 0.1 m is discretized using an "O" type mesh shown schematically in Fig. 2. The time variation of the induced current at $\theta = 0^o$ on the cylinder surface, J_y, is shown in Fig. 3 with different spatial accuracy for a conventional single level implementation and compared with that obtained through inverse discrete Fourier transform (IDFT) of frequency domain solution and time domain integral equation (TDIE) based solutions in Ref. [17]. FVTD results tend to be good for at least second-order accuracy with second and third-order accurate results overlapping and the induced current peaking at the correct time. Fig. 4, compares result obtained with a conventional third-order accurate implementation and that using a three-level method with $\nu = 1,10$. The results match exactly, testifying to the transient accuracy of the multilevel method measured in terms of time variation of the induced current J_y for this problem, even in its frozen τ variant with $\nu = 10$ implying ten explicit time steps at the lowest first-order accurate level.

The next numerical simulation involved calculating the radar cross section (RCS) or scattering width in 2D, of a perfectly conducting circular cylinder. Computations were performed for total time corresponding to a fixed number of time periods of the incident harmonic wave after which the bistatic RCS (σ) is computed using a near-to-far field transformation. A discussion on the number of incident wave periods to be time-stepped for attaining sinusoidal steady state in a FDTD framework under harmonic incident excitation as attempted here is presented in Ref. [9]. The number of incident time periods leads to T in Eq. (2.40) and fixes N with Δt limited by usual stability considerations. The problem considered has the circular cylinder subject to continuous harmonic incident TM illumination with a/λ=4.8, where a is the cylinder radius and λ the wavelength of the incident wave [11,12]. Results are uniformly shown after time-stepping 6 incident wave pe-

https://doi.org/10.4208/cicp.181113.271114a Published online by Cambridge University Press

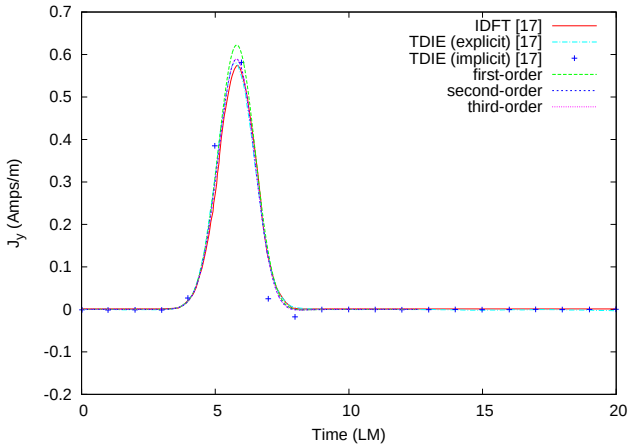


Figure 3: Induced current J_y at $\theta = 0^o$, TE Gaussian plane wave, different orders of accuracy.

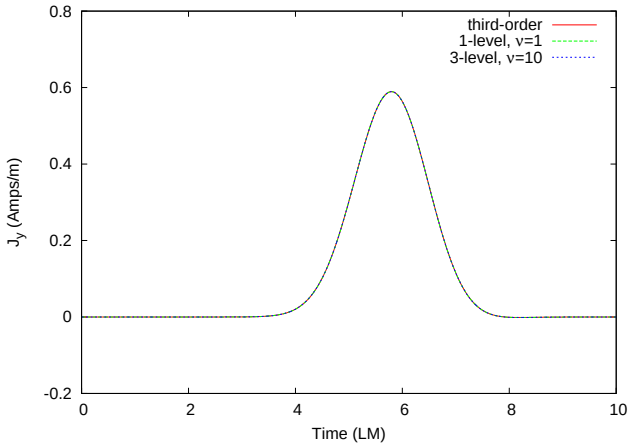


Figure 4: Induced current J_y at $\theta = 0^o$, TE Gaussian plane wave, comparison of single and multilevel results.

riods which was found to be adequate for desired steady state response in such problems for the electrical sizes under consideration. Fig. 5, shows σ for a conventional single level implementation for different spatial orders of accuracy on an "O" grid with 300 points in the circumferential direction corresponding to a resolution of 10 PPW on the scatterer surface. The number of points in the radial direction is 50. Average mesh resolution in terms of PPW in the circumferential and radial directions are respectively 6.42 and 4.16. The relatively lower resolution of 10 PPW on the cylinder surface is deliberately chosen to bring out the effect of the numerical discretization error on the solution obtained using different spatial orders of accuracy from fourth to first. The highest fourth-order accurate solutions are closest to the exact solution with first and second-order accurate solutions showing significant deviation away from near-specular-regions. The monostatic point is

https://doi.org/10.4208/cicp.181113.271114a Published online by Cambridge University Press

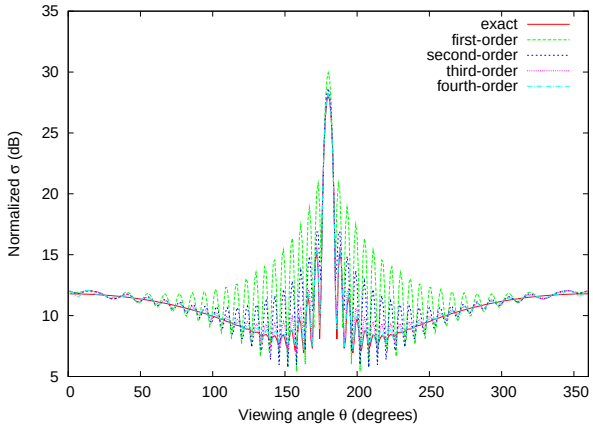


Figure 5: Bistatic RCS $a/\lambda = 4.8$, continuous harmonic TM illumination, different orders of accuracy, single level.

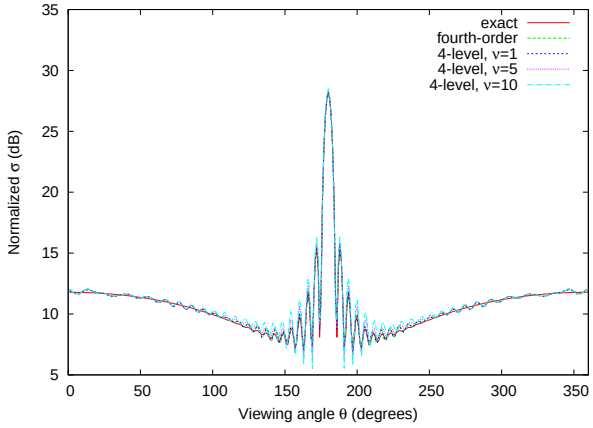


Figure 6: Bistatic RCS $a/\lambda = 4.8$, continuous harmonic TM illumination, comparison of single and multilevel results.

located at 0^o in the bistatic plot. The errors in σ are quantified and presented in Table 1. The errors are defined as

$$L_2(\sigma) = \sqrt{\frac{\sum_{l=1}^{L}[\sigma(\theta_l) - \sigma_e(\theta_l)]^2}{\sum_{l=1}^{L}[\sigma_e(\theta_l)]^2}} \tag{3.7}$$

and

$$L_\infty(\sigma) = \frac{\max_l |\sigma(\theta_l) - \sigma_e(\theta_l)|}{\max_l |\sigma_e(\theta_l)|} \tag{3.8}$$

with $\theta_l = 2\pi\frac{l}{L}$ the viewing angle, $0 \geq \theta \geq 2\pi$. σ and σ_e respectively represent the computed and exact values for the bistatic RCS.

In Fig. 6, results for σ obtained using a four-level method are compared with a conventional fourth-order spatially accurate solution on the same grid corresponding to 10 PPW

https://doi.org/10.4208/cicp.181113.271114a Published online by Cambridge University Press

Table 1: Errors in σ, single level.

Order (p)	$L_2(\sigma)$	$L_\infty(\sigma)$
1	2.5×10^{-1}	3.9×10^{-1}
2	1.2×10^{-1}	2.2×10^{-1}
3	3.8×10^{-2}	6.6×10^{-2}
4	1.7×10^{-2}	2.9×10^{-2}

Table 2: Errors in σ, four-level.

Scheme	$L_2(\sigma)$	$L_\infty(\sigma)$
conventional fourth-order	1.7×10^{-2}	2.9×10^{-2}
four-level $(\nu=1)$	1.5×10^{-2}	2.3×10^{-2}
four-level $(\nu=5)$	2.2×10^{-2}	3.1×10^{-2}
four-level $(\nu=10)$	3.5×10^{-2}	5.2×10^{-2}

on the scatterer surface along with exact solutions. Results for the multilevel method are shown for $\nu=1,5,10$. As can be seen in the results in Fig. 6, it is possible to execute almost 5 to 10 explicit time steps on the lowest first-order level of the four-level multilevel scheme during each cycle without major deviation from conventional fourth-order spatially accurate results. The four-level scheme in its sawtooth variation ($\nu=1$) almost exactly replicates the conventional fourth-order accurate result. This is also substantiated quantitatively when the errors, as defined in Eqs. (3.7) and (3.8), are compared for the four-level multilevel scheme and conventional fourth-order spatially accurate solutions in Table 2. In fact the four-level multilevel scheme in its sawtooth variation is slightly more accurate than the conventional fourth-order scheme. This can be attributed to overall reduced stencil excursions in the ENO context for the four-level multilevel scheme compared to the conventional fourth-order accurate scheme. We also consider the case of a perfectly conducting NACA 0012 airfoil shown schematically in Fig. 7, illuminated

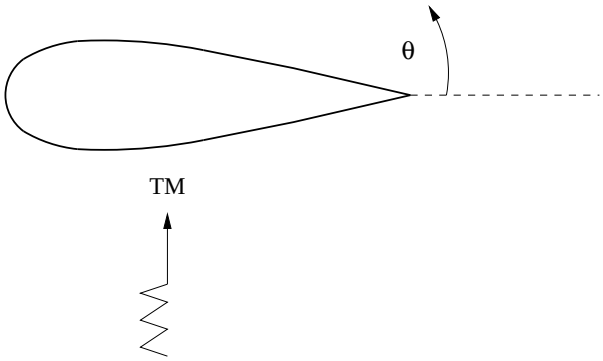


Figure 7: Airfoil illumination, schematic.

https://doi.org/10.4208/cicp.181113.271114a Published online by Cambridge University Press

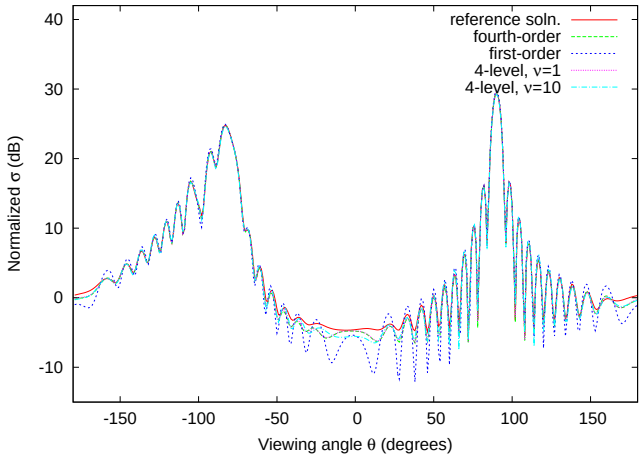


Figure 8: Bistatic RCS $a/\lambda=10$, continuous harmonic TM illumination, comparison of single and multilevel results.

on the broadside by a continuous harmonic incident TM wave. Bistatic RCS results are shown for $a/\lambda=10$ as in Refs. [11, 12, 18], where a indicates the airfoil chord length. A body fitted grid is employed with a topology identical to that used for the circular cylinder. Fig. 8 compares conventional single level solution of fourth and first-order spatial accuracy with that obtained from a four-level method and a reference solution. The conventional and multilevel solutions are obtained on a grid with only 50 cells on the airfoil surface after 6 incident wave periods. The four-level multilevel solutions are for $\nu=1$ and $\nu=10$. The reference solution is obtained on a very fine mesh with 1600 cells on the airfoil surface after 10 incident wave periods. As in the case of the circular cylinder, the four-level solution with $\nu=1$ is almost identical to the conventional fourth-order accurate approximation while the frozen variant with $\nu=10$ shows only minor deviation.

3.2 Computational efficiency

To get an idea of the savings incurred in CPU time we consider a m level multilevel method with $\nu=\nu_m$ and an uniform time step Δt at all levels. We assume that a p^{th} order spatially accurate approximation is uniformly k times more expensive than the corresponding $(p-1)^{th}$ order approximation. With this assumption the number of work units (WU) for advancing $(m-1+\nu_m)\Delta t$ in time is

$$1+\frac{1}{k}+\frac{1}{k^2}+\cdots+\frac{1}{k^{m-2}}+\frac{\nu_m}{k^{m-1}}, \tag{3.9}$$

where one WU is defined as the computational work incurred by the highest (m^{th}) order accurate approximate method in advancing time Δt. Thus, the computational effort incurred per time step excluding overheads, for the m-level multilevel method is less than

https://doi.org/10.4208/cicp.181113.271114a Published online by Cambridge University Press

a conventional single level implementation of m^{th} order spatial accuracy scheme by a factor of

$$\frac{\sum_{p=1}^{m-1} k^p + \nu_m}{(m-1+\nu_m)k^{m-1}}. \tag{3.10}$$

The overheads in the multilevel method are not significant and are mainly from the calculation of the $\boldsymbol{R}_p(\boldsymbol{U}^{n-1})$ contribution to the evaluation of the relative truncation error $\boldsymbol{\tau}_p^n$ in Eq. (2.31). There are no explicit restriction or prolongation operations required. Based on Eq. (3.10) the computational cost for a four level method ($m=4$) with $\nu_m=10$ and $k=2$ which is a reasonable assumption in the current context [19], turns out to be approximately 3/13 times that of a conventional fourth-order spatially accurate method. In the present work it implies fourth-order spatial accuracy being achieved at approximately the cost of the second-order spatially accurate operator or at 2 times that of a first-order accurate operator. Thus, the computational cost of achieving higher-order spatial accuracy for solving problems of linear wave propagation in the proposed multilevel framework is comparable to that of lower-order operators. The cost advantage of the proposed multilevel method can also be expressed as that of achieving highest m-order spatial accuracy at reduced computational costs comparable to that for a lower-order accurate operator $p<m$ on a fixed Ω^h.

4 Conclusion

The FVTD technique is solved in an algebraic multilevel framework which allows higher-order accuracy to be inexpensively enforced by the use of an appropriate forcing function while cycling the solution through coarser spatial approximations. This method is more generally applicable to sufficiently smooth solutions in linear wave propagation which includes solutions of the time-domain Maxwell's equations for electromagnetic scattering problems. The proposed multilevel method does not require restriction or prolongation operators and blends easily with a higher-order FVTD based framework for solving the time-domain Maxwell's equations. Higher-order transient as well as steady-state results can be obtained at a fraction of the computational cost of a conventional higher-order FVTD implementation, and at costs comparable to that for lower-order methods. Results have been presented for multilevel cycles in sawtooth and frozen τ variants where more than one explicit time step is performed at the lowest approximation level. As in the well established case of multigrid methods, many other variants may be possible in the present multilevel framework leading to further reduction in CPU time.

References

[1] J.S. Hesthaven, Higher-order accurate methods in time-domain electromagnetics: A review, Adv. in Imaging and Electron Phys., 127(2003), 59-123.

https://doi.org/10.4208/cicp.181113.271114a Published online by Cambridge University Press

[2] A.V. Kabakian, V. Shankar and W.F. Hall, Unstructured grid-based discontinuous Galerkin method for broadband electromagnetic simulations, J. Sci. Comput., 20(2004), 405-431.
[3] K.S. Yee and J.S. Chen, The finite-difference time domain (FDTD) and finite-volume time-domain (FVTD) methods in solving Maxwell's equations, IEEE Trans. Antennas and Propagation, 45(1997), 354-363.
[4] C.W. Manry, S.L. Broschat and J.B. Schneider, Higher-order FDTD methods for large problems, ACES J., 10(1995), 17-29.
[5] A. Brandt, Multi-level adaptive solutions to boundary value problems, Math. Comp., 31(1977), 333-390.
[6] A. Brandt, Guide to multigrid development, in Springer Lecture Notes in Mathematics 960, Springer-Verlag, Berlin 1982.
[7] K.J. Fidkowski, T.A. Oliver. J. Lu and D.L. Darmofal, *p*-Multigrid solution of higher-order discontinuous Galerkin discretizations of the compressible Navier-Stokes equations, J. Comp. Phys., 207(2005), 92-113.
[8] W.L. Briggs, V. E. Henson and S.F. McCormick, A Multigrid tutorial, 2^{nd} edition, SIAM, 2000.
[9] A. Taflove and K.R. Umashankar, Review of FD-TD numerical modeling of electromagnetic wave scattering and radar cross section, Proc. of the IEEE, 77(1989), 682-699.
[10] W.L. Wan and T.F. Chan, A phase error analysis of multigrid methods for hyperbolic problems, SIAM J. Sci. Comput., 25(2003), 857-880.
[11] N.Deore and A. Chatterjee, A cell-vertex based multigrid solution of the time domain Maxwell's equations, PIER B, 23(2010), 181-197.
[12] A. Chatterjee and R.-S. Myong, Efficient implementation of higher-order finite volume time domain method for electrically large scatterers, PIER B, 17(2009), 233-254.
[13] R.V. Chima, E. Turkel and S. Schaffer, Comparison of three explicit multigrid methods for the Euler and Navier-Stokes equations, AIAA Paper, 87-0602(1987).
[14] C.W. Shu and S. Osher, Efficient implementation of essentially non-oscillatory shock-capturing schemes, J. Comp. Phys., 77(1988), 439-471.
[15] C. W. Shu and S. Osher, Efficient implementation of essentially non-oscillatory shock-capturing schemes II, J. Comp. Phys., 83(1989), 32-78.
[16] A. Chatterjee and A. Shrimal, Essentially nonoscillatory finite volume scheme for electromagnetic scattering by thin dielectric coatings, AIAA J., 42(2004), 361-365.
[17] S.M. Rao, D.A. Vechinski and T.K. Sarkar, Infinite conducting cylinders: TDIE solution, in Time domain electromagnetics, Academic Press, 1999
[18] V. Shankar, W.F. Hall and A.H Mohammadian, A time-domain differential solver for electromagnetic scattering problems, Proceedings of the IEEE, 77(1989), 709-721.
[19] J. Casper, C-W Shu and H.L. Atkins, A comparison of two formulations for higher-order accurate essentially non-oscillatory schemes, ICASE report number 93-27, 1993.

https://doi.org/10.4208/cicp.181113.271114a Published online by Cambridge University Press